# マウス脊髄におけるGABA除去システムの発達変化について

**Characteristic development of the GABA-removal system in the mouse spinal cord**

**Jeongtae Kim, Yoshinori Kosaka, Chigusa Shimizu-Okabe, Aya Niizaki, and Chitoshi Takayama***

Department of Molecular Anatomy, School of Medicine, University of the Ryukyus, Uehara 207, Nishihara, Okinawa, 9030215, Japan

**Section: Cellular and Molecular Neuroscience**

**Section Editor: Doctor Robert Hevner**

***Corresponding Author**

Department of Molecular Anatomy, School of Medicine, University of the Ryukyus, Uehara 207, Nishihara, Okinawa, 9030215, Japan

Phone: +81-98-895-1105

Fax: +81-98-895-1401

E-mail: takachan@med.u-ryukyu.ac.jp

**Abstract**

Gamma-amino butyric acid (GABA) is a predominant inhibitory neurotransmitter in the central nervous system (CNS). Released GABA is removed from the synaptic cleft by two GABA transporters (GATs), GAT-1 and GAT-3, and their dysfunction affects brain functions. The present study aimed to reveal the ontogeny of the GABA-removal system by examining the immunohistochemical localization of GAT-1 and GAT-3 in the embryonic and postnatal mouse cervical spinal cord. In the dorsal horn, GAT-1 was localized within the presynapses of inhibitory axons after embryonic day 15 (E15), a little prior to GABAergic synapse formation. The GAT-1-positive dots increased in density until postnatal day 21 (P21). By contrast, in the ventral horn, GAT-1-positive dots were sparse during development, although many transient GABAergic synapses were formed before birth. GAT-3 was first localized within radial processes of radial glia in the ventral part on E12 and the dorsal part on E15. The initial localization of the GAT-3 was almost concomitant with the distribution of GABAergic neurons. GAT-3 continued to be localized within the processes of astrocytes, and increased in expression until P21. These results suggested the following: (1) Before synapse formation, GABA may be transported into the processes of radial glia or immature astrocytes by GAT-3. (2) At the transient GABAergic synapses in the ventral horn, GABA may not be reuptaken into the presynapses. (3) In the dorsal horn, GABA may start to be reuptaken by GAT-1 a little prior to synapse formation. (4) After synapse formation, GAT-3 may continue to remove GABA from

immature and mature synaptic clefts into the processes of astrocytes. (5) Development of the GABA-removal system may be completed by P21.

**Key words**

astrocyte, GABA transporter 1 (GAT-1), GABA transporter 3 (GAT-3), GABAergic synapse, radial glia, vesicular GABA transporter (VGAT)

**Highlights**

**1.** We examined the ontogeny of GABA-removal system in the mouse spinal cord.

**2.** GABA may be removed to radial glia-astrocyte lineage cells by GAT-3.

**3.** GABA may not be reuptaken to the presynapses in the ventral horn.

**4.** GABA reuptake may start a little prior to synapse formation in the dorsal horn.

**5.** Development of the GABA-removal system may be completed by P21.

**Abbreviations**

ABC: avidin-biotin-peroxidase-complex
AF: anterior funiculus
As: astrocyte
Ax: axon
cc: central canal
CNS: central nervous system
DH: dorsal horn
E: embryonic day
f: presynapse containing flat vesicles
GABA: γ-amino butyric acid
GAT: GABA transporter
GAD: glutamic acid decarboxylase
GLAST: glutamate-aspartate transporter
Gly: glycine
LF: lateral funiculus
M: month old
ML: mantle layer
MZ: marginal zone
NRS: normal rabbit serum
P: postnatal day
PB: phosphate buffer
PF: posterior funiculus
R: $GABA_A$ receptor and glycine receptor
RG: radial glia
s: presynapse containing spherical vesicles
VGAT: vesicular GABA transporter
VH: ventral horn
VZ: ventricular zone
WM: white matter
I-IV: lamina I to IV in the dorsal horn

**Contributors**

The majority of the experiments were done by **JK** and **YK**. Double staining was performed by **CS**, and electron microscopic analysis was done by **AN** and **CT**. Figure plates and tables were organized by **JK**, **YK**, **CS**, and **CT**. The text was written by **JK** and **CT,** and checked by all authors.

## 1. Introduction

Gamma-amino butyric acid (GABA) is an important neurotransmitter in the adult central nervous system (CNS) (Olsen and Tobin, 1990, Macdonald and Olsen, 1994). After release from presynaptic terminals, GABA binds to the GABA receptors on the postsynaptic membrane and is rapidly transported into the presynaptic terminals and glial processes surrounding the synapses by the GABA transporters (GATs), GAT-1 and GAT-3 (Jursky et al., 1994, Kanner, 1994, Borden, 1996, Gadea and Lopez-Colome, 2001, Takayama, 2005). The establishment of this removal system is one of the most important steps in synapse formation and is crucial for the maintenance of normal GABAergic transmission. The dysfunction of these transporters affects brain functions and causes various diseases, such as ataxia, depression, hypoalgesia, and tremor (Chiu et al., 2005, Liu et al., 2007a, Liu et al., 2007b, Xu et al., 2008, Zink et al., 2009, Egawa et al., 2012, Shi et al., 2012).

Previous studies have investigated the ontogeny of the GABA-removal system in various brain regions by *in situ* hybridization (Evans et al., 1996) and immunohistochemistry (Jursky et al., 1994, Jursky and Nelson, 1999, Minelli et al., 2003b, Vitellaro-Zuccarello et al., 2003, Takayama and Inoue, 2005, Avila et al., 2011) for the GABA transporters, GAT-1, GAT-2, and GAT-3. Distinct types of GABA transporters were localized during development of each region, but, as demonstrated in the adult mouse, GAT-1 was commonly localized in presynapses

and GAT-3 was located in astrocytic processes (Radian et al., 1990, Minelli et al., 1995, Itouji et al., 1996, Minelli et al., 1996, Morara et al., 1996, Jin et al., 2011a, Jin et al., 2011b).

We have previously investigated the developmental changes in GABA signaling in the CNS (Takayama and Inoue, 2004c, b, a, 2005, 2006, 2007, 2010). We have also examined the time course of GABAergic neuron localization, GABAergic synapse formation, and GABA action in the spinal cord (Kosaka et al., 2012). In the present study, we focused on the developmental changes in the GABA-removal system in the spinal cord, because the GABA-removal system is crucial for the maintenance of motor and sensory functions (Chiu et al., 2005, Xu et al., 2008). Although previous studies have demonstrated GAT-1 and GAT-3 expression and localization in the embryonic spinal cord (Jursky and Nelson, 1996), changes in cellular and subcellular localization of the transporters and their spatial and temporal relationship with the formation of GABAergic networks were not clearly revealed.

In the present study, to reveal the development of the GABA-removal system and its special relationship to the development of GABAergic networks, we used light- and electron-microscopy to examine the changes in expression and localization of GAT-1 and GAT-3 in the embryonic and postnatal mouse spinal cord. We found that GAT-1 was localized within presynapses in the dorsal horn a little prior to the synapse formation, but not in the ventral horn, although many GABAergic synapses were transiently formed in the ventral horn, namely transient GABAergic synapses (Wu et al., 1992, Gao et al., 2001, Tran et al., 2003, Allain et al.,

2006, Sibilla and Ballerini, 2009, Kosaka et al., 2012). GAT-3 was localized in the processes of radial glia-astrocyte linage cells, after GABAergic neurons were localized. Development of the GABA-removal system may be completed by P21.

## 2. Experimental Procedures

### 2.1. Animals

Male mice on postnatal day (P) 0, P7, P14, P21, and 2-month-old mice (P2M), and pregnant mice (C57Bl/6J) were used in this study. Adult and pregnant mice were deeply anesthetized by intra-peritoneal injection of a mixed solution (10 μl/g body weight), containing 8% Nembutal and 20% ethanol in saline. Fetuses on embryonic day (E) 12 (E0 = mating day), E13, E15, E16, and E18 were removed from the uterus of pregnant mice. At least five mice or fetuses were investigated for immunostaining at each stage.

These experiments were approved by the Animal Care and Use Committees of the University of the Ryukyus (No. 5539) and were performed in compliance with the Guide for the Care and Use of Laboratory Animals of the University of the Ryukyus. Every effort was made to minimize the number of animals and their suffering.

### 2.2. Antibody characterization

Characterization of all antibodies used in the present study is listed in Table 1. The specificity of the VGAT antibody was examined in the previous study (Takayama and Inoue, 2004c). To test the specificity of GAT-1 and GAT-3 immunolabeling, we performed the

immunostaining with normal rabbit serum (diluted 1:10000) instead of GAT-1 or GAT-3 antibody. No obvious staining was detected in the spinal cord on P2M and E15 (Data not shown).

**2.3. Tissue preparation and immunohistochemistry for light microscopic analysis**

Fetuses on E12 were immediately immersed in fixatives containing 4% paraformaldehyde in phosphate buffer (PB, 0.1 M, pH 7.4). Fetuses on E13, E15, E16, E18, and adult mice were fixed by transcardial perfusion with the same fixative. After immersion in the same fixative overnight, the fetuses and spinal cord of postnatal mice were cryoprotected with 30% sucrose in PB for 2 days, and cut into 20 μm-thick transverse sections with a cryostat. The sections of the cervical enlargement were mounted on glass slides coated with gelatin and immunostained. Sections were incubated methanol containing 0.3% $H_2O_2$ for 30 min, PB for 10 min, 3% normal goat serum in PB for 1h, and GAT-1 and GAT-3 antibodies as previously described (Takayama and Inoue, 2005). After rinsing three times with PB for 15 min, sections were visualized using the avidin-biotin-peroxidase complex (ABC) method (Histofine kit; Nichirei, Tokyo, Japan) (Hsu et al., 1981), and were observed by a light microscopy (Olympus AX-80).

For double staining, sections incubated with GAT-1 or GAT-3 antibodies were visualized with anti-rabbit IgG, conjugated to Alexa Fluor 568 (Life Technologies, Carlsbad, CA). After rinsing three times in PB, sections were incubated with a guinea pig VGAT antibody (Takayama and Inoue, 2004a) or a mouse nestin antibody (Millipore, Billerica, MA) and

visualized using anti-guinea pig IgG conjugated to Alexa Fluor 488 (Life Technologies, Carlsbad, CA) or anti-mouse IgG conjugated to Alexa Fluor 488, respectively. The immunofluorescence images were observed by a laser scanning confocal microscope (Olympus FV 1000).

### 2.4. Tissue preparation and immunohistochemistry for electron microscopic analysis

P2M mice and fetuses on E15 and E18 were fixed by transcardial perfusion with 4% paraformaldehyde in PB. After immersion in the same fixative overnight, cervical spinal cords were cut into 300 μm-thick transverse sections using a microslicer (Dosaka, Kyoto, Japan). Sections were incubated in 3% normal goat serum for 1h, followed by primary antibodies against GAT-1 or GAT-3 overnight at room temperature. After visualization using the ABC method (Hsu et al., 1981), sections were post-fixed with 1% glutaraldehyde in PB for 20 min and 1% $OsO_4$ in PB for 2 h at 4°C, stained with 1% uranyl acetate aqueous solution overnight, and embedded in epoxy resin in the usual manner (Takayama and Inoue, 2004a). Ultra-thin sections were observed under an electron microscope (H-9500, Hitachi, Tokyo, Japan). Figure plates were prepared by using Adobe Photoshop**.**

## 3. Results

### 3.1. Immunohistochemical localization of GAT-1 and GAT-3 in the adult mouse spinal cord

First, we examined the light- and electron-microscopic localization of GAT-1 and GAT-3 in the cervical enlargement of the spinal cord of 2-month-old mice. Dense GAT-1

immunolabeling was detected as fine dots in laminae I, II, and III in the dorsal horn (Fig. 1A). In the ventral horn, the GAT-1-positive dots were sparse and the neuropil was weakly stained (Fig. 1B). Electron microscopic analysis revealed that the GAT-1 immunolabeling was localized near the cell membrane of the presynapses, which contained many flat vesicles and often formed symmetric synapses with dendrites (Fig. 1C), indicating that GAT-1 was mainly localized at the presynaptic terminals of inhibitory axons. Furthermore, a small amount of immunolabeling was detected within non-neuronal structure (arrowheads in Fig. 1C) as demonstrated in other regions (Minelli et al., 1995, Takayama and Inoue, 2005, Jin et al., 2011a, Jin et al., 2011b). The structure may be processes of astrocytes since it filled up the inter-neuronal regions as previously described (Peters et al., 1991).

GAT-3 immunolabeling was diffusely detected in the neuropil throughout the gray matter, including both the dorsal horn (Fig. 1D) and the ventral horn (Fig. 1E). Electron microscopic analysis revealed that dense GAT-3 immunolabeling filled up the inter-neuronal space surrounding the symmetric and asymmetric synapses (Fig. 1F), as previously reported in other regions of the CNS (Minelli et al., 1996, Minelli et al., 2003a, Takayama and Inoue, 2005, Jin et al., 2011a, Jin et al., 2011b). The structure may be also processes of astrocytes since it filled up the inter-neuronal regions as previously described (Peters et al., 1991).

These results suggested that GABA may be transported into presynapse by GAT-1 and astrocytic processes mainly by GAT-3 in the adult spinal cord as demonstrated in other regions

(Radian et al., 1990, Minelli et al., 1995, Itouji et al., 1996, Minelli et al., 1996, Morara et al., 1996, Jin et al., 2011a, Jin et al., 2011b).

### 3.2. Developmental localization of GAT-1 in the spinal cord

GAT-1 was first detected in the anterior part of the marginal zone on E12 (Fig. 2A). The faint immunolabeling spread to the lateral funiculus on E13 (Fig. 2B) and the posterior funiculus on E15 (Fig. 2C). The dorsal horn was weakly stained on E15 and the immunolabeling gradually increased in density and intensity on E16 (Fig. 2D) and E18 (Fig. 2E). In contrast, the signal was faint in the ventral horn during embryonic development (Fig. 2). In the higher magnification view, a few GAT-1-positive dots were localized within the marginal zone on E13 (Fig. 3A) and E15 (Fig. 3B). Within the ventral horn, GAT-1-positive dots were detected on E16 (Fig. 3C) and E18 (Fig. 3D), but were sparse compared with VGAT- or glutamic acid decarboxylase (GAD)-positive dots on the same embryonic day (Kosaka et al., 2012). In the posterior funiculus, many GAT-1-positive dots were moderately and clearly localized on E15 (Fig. 3E) through E18, and their density and immunolabeling intensity were much higher than those in the anterior funiculus. In the dorsal horn, GAT-1 immunolabeling was detected at axon varicosities and axons on E15 (Fig. 3F). The density of the GAT-1-positive varicosities gradually increased after E16 (Fig. 3G and 3H), and numerous dots were localized mainly in lamina III of the dorsal horn on E18 (Fig. 3H). Furthermore, to characterize the GAT-1-positive profiles in the developing spinal cord, we examined the electron microscopic localization. On E18, GAT-1

immunolabeling was localized within the presynaptic terminals, which contained flat vesicles (Fig. 4A-C), and adjacent axons in the dorsal horn (Fig. 4C). A small amount of immunolabeling was detected within processes of astrocytes in the embryonic spinal cord as detected in the adult mice (arrowheads in Fig. 4).

After birth, the neuropil was weakly stained in the ventral horn and few GAT-1-positive dots were detected (Fig. 5A-D). In the dorsal horn, in contrast, GAT-1 immunolabeling was increased in intensity after birth (Fig. 5E-H). On P0 (Fig. 5E), the densely stained GAT-1-positive dots were mainly localized in lamina III. Lamina I was labeled on P7 (Fig. 5F), and lamina II was positive after P14 (Fig. 5G and 5H). Staining intensity and density markedly increased between P7 (Fig. 5F) and P14 (Fig. 5G), and slightly increased until P21 (Fig. 5H). During postnatal development, the neuropil was also weakly GAT-1- immunolabeled (Fig. 5).

These results indicated that GAT-1 was mainly localized within the presynapses in the dorsal horn after E15, and increased in expression until P21.

### 3.3. Developmental localization of GAT-3 in the spinal cord

GAT-3 immunolabeling was first detected in the ventral region on E12 (Fig. 6A). On E13, immunolabeling in the ventral region was detected in the radial fibers extending from the central canal to the pial surface (Fig. 6B). In particular, radial fibers were heavily stained in the white matter. On E15, the labeled fibers were localized throughout the spinal cord, and the intensity and density of the immunolabeling was markedly increased within gray matter (ventral

horn) (Fig. 6C). On E16 (Fig. 6D) and E18 (Fig. 6E), fibers were not clearly discernible within the gray matter, and the GAT-3 immunolabeling exhibited small fragments that occupied the neuropil. In contrast, radial fibers were densely labeled in the white matter. In the ventral portion at higher magnification, weak GAT-3 immunolabeling was localized to several radial fibers extending from the central canal to the pial surface on E12 (Fig. 7A). On E13, numerous radial fibers were clearly labeled (Fig. 7B). In the gray matter, weak to moderate GAT-3-immunolabeling was detected in the radial processes, which had few branches. In the white matter, processes were densely labeled, and end feet were clearly discernible (Fig. 7B). On E15, intensity of the GAT-3 immunolabeling markedly increased in the ventral horn and the labeled radial fibers had many branches (Fig. 7C). On E16, radial processes were unclear and numerous fragments or particle-like-profiles were scattered among large motor neurons (Fig. 7D). On E18, dots and short fibrous fragments occupied the neuropil, which may have contributed to filling up the inter-neuronal space (Fig. 7E). In the dorsal horn, radial processes were first detected on E13 (Fig. 7F). The shapes of GAT-3-positive structure gradually changed to fragment-like profiles on E16 (Fig. 7G), and small dots scattered in the neuropil in laminar II and III on E18 (Fig. 7H). To further characterize the GAT-3-positive profiles in the developing spinal cord, we examined the localization using electron microscopy on E15 (Fig. 8A-D) and E18 (Fig. 8E and 8F). GAT-3 was localized within the radial fibers extending straight to the pia mater, and their short branches invading into the inter-neuronal space on E15 (Fig. 8A-D). On E18, GAT-3 was localized near

the plasma membrane of astrocyte-like cells (Fig. 8E), and the GAT-3-positive processes were localized near the symmetric and asymmetric synapses (Fig. 8E and 8F).

After birth, GAT-3 immunolabeling increased in intensity and density until P21, but radial processes were not detected in either the ventral (Fig. 9A-D) or the dorsal horns (Fig. 9E -H). On P0, fine dots or short fibrous profiles occupied the neuropil region among the large motor neurons in the ventral horn (Fig. 9A). On P7, the immunolabeling increased in intensity and density (Fig. 9B). On P14 and P21, the neuropil was diffusely occupied by GAT-3 immunolabeling (Fig. 9C and 9D). In the dorsal horn on P0, GAT-3 immunolabeling was detected in all lamina including lamina I, and exhibited fine dots (Fig. 9E). Density of the GAT-3-positive dots markedly increased during the first postnatal week (Fig. 9F) and gradually increased until P21 (Fig. 9G and 9H). The neuropil was occupied by GAT-3 immunolabeling in the dorsal horn on P21 (Fig. 9H).

These changes in the shape of GAT-3-positive profiles, detected by the light microscopy, were quite similar to those of radial glia-astrocyte lineage cells, detected by immunohistochemistry for RC1, nestin, and glutamate-aspartate transporter (GLAST) (Shibata et al., 1997, Liu et al., 2002). Furthermore, electron microscopic analysis revealed the following: (1) Localization of chromatin within nuclei of GAT-3-positive cells was characteristic for astrocytes (Peters et al., 1991). (2) GAT-3 was not detected within the neuronal elements, such as dendrites, terminals, and axons. (3) GAT-3-positive profiles filled up the inter-neuronal spaces.

These results suggested that GAT-3 may be localized to the radial glia and astrocytes in the ventral part of the cervical spinal cord after E12 and the plasma membrane of astrocytic processes in the dorsal horn after E15.

### 3.4. Double labeling of GAT-1 and GAT-3 with synaptic and glial markers, VGAT, and nestin

To reveal the spatial and temporal relationship between GAT-1 expression and synapse formation, we examined the double staining with VGAT, which is a marker of inhibitory synaptic vesicles in both GABAergic and glycinergic synapses. In the dorsal horn on E18, many GAT-1-positive dots were colocalized with VGAT, but not fully merged (Fig. 10A). Many GAT-1-positive but VGAT-negative dots were also detected in the same image (Fig. 10A), indicating that GAT-1 was localized to the inhibitory terminals during embryonic period, but the onset of the GAT-1 expression was a little prior to synapse formation. By contrast, in the ventral horn, although VGAT-positive dots were numerous, few GAT-1-positive dots were colocalized with VGAT (circles in Fig. 10B). These results indicated that GAT-1 was localized to the inhibitory terminals which may remain as the presynapses of permanent GABAergic synapses in the dorsal horn, but was not localized to the transient GABAergic synapses in the ventral horn.

Next, to reveal the temporal relationship between GAT-3 localization and development of radial glia-astrocyte lineage cells, we examined the double labeling with nestin, which is the intermediate filament in the neural stem cells or radial glia in the developing CNS. In the ventral

horn on E13, the trunk of the GAT-3-positive fibers colocalized with nestin, while the branches were GAT-3-positive but nestin-negative (Fig. 10C). In the dorsal horn on E13, many radial fibers were nestin-positive but GAT-3-negative (Fig. 10D). In the dorsal horn on E15, a few nestin-positive fibers were colocalized with GAT-3 immunolabeling, but many GAT-3-positive profiles were nestin-negative (Fig. 10E). These results indicated that radial glia did express GAT-3, but early stage of radial glia did not express GAT-3, and suggested that GAT-3 may be expressed in the processes of radial glial development and continue to be localized in the astrocytes.

Furthermore, to examine the positional relationship between astrocytic processes and inhibitory terminals, we performed double labeling with VGAT. Some of the VGAT-positive dots were attached to the GAT-3-positive fibrous profiles, but many VGAT-positive dots were detected among the GAT-3-positive profiles (Fig. 10F), indicating that GAT-3-positive astrocytes did not yet completely seal the synapses on E18.

## 4. Discussion

In the present study, we examined the immunohistochemical localization of GAT-1 and GAT-3 in the embryonic and postnatal mouse spinal cord, and revealed the characteristic development of the GABA-removal system. The results are summarized in Figure 11.

### 4.1. Developmental changes in the GABA-removal system in the mouse spinal cord

Previous studies demonstrated the early distribution of GABAergic neurons before

synapse formation in the rodent spinal cord (Wu et al., 1992, Schaffner et al., 1993, Phelps et al., 1999, Tran et al., 2003, Sibilla and Ballerini, 2009, Kosaka et al., 2012), suggesting that GABA may be extrasynaptically released for several days, and play an important role in morphogenesis of the CNS (Ben-Ari, 2002, McCarthy et al., 2002, Owens and Kriegstein, 2002, Represa and Ben-Ari, 2005, Ben-Ari et al., 2007). The present study demonstrates that GAT-3 was localized to the radial fibers during this developmental period. These results suggested that GAT-3 may exclusively transport extrasynaptically released GABA into the radial glia or immature astrocytes (Fig. 11A).

In the ventral horn, a large number of GABAergic synapses are formed during late embryonic development (Wu et al., 1992, Gao et al., 2001, Tran et al., 2003, Allain et al., 2006, Sibilla and Ballerini, 2009, Kosaka et al., 2012), but many of these synapses eventually disappeared. Several previous studies suggested the possibility that transient GABAergic synapses might be transformed into glycinergic synapses (Gao and Ziskind-Conhaim, 1995, Nabekura et al., 2004), but the fate of these transient GABAergic synapses was still unknown. The present study demonstrated that, except for a few, GAT-1 was not detected in the presynapses at these transient GABAergic synapses in the ventral horn, suggesting that only GAT-3 removes GABA into astrocytes (Fig. 11B).

In the dorsal horn, conversely, GAT-1 appeared during synapse formation. The onset was a little earlier than that of VGAT (Fig. 10A). This result suggested that GABA released in

the immature synaptic cleft or extracellular space, which was partially sealed by astrocytic processes, may be transported to the astrocytic processes by GAT-3, and be reuptaken to the developing presynapse by GAT-1 (Fig. 11C). Finally, both GATs may remove GABA from the synaptic cleft (Fig. 11D).

**4.2. Regional difference in the development of the GABA-removal system in the CNS**

Developmental changes in the GABA-removal system in the spinal cord, demonstrated in the present study, were characteristic in comparison with those in other regions as described below. First, GABA may be removed by GAT-3 to the astrocytic processes before formation of GABAergic synapses. In the cerebellar cortex, no immunolabeling was detected before synapse formation (Takayama and Inoue, 2005). In the cerebral cortex, GAT immunolabeling before birth was weak to faint except for in the marginal zone (Jursky and Nelson, 1996, Minelli et al., 2003b, Vitellaro-Zuccarello et al., 2003, Conti et al., 2004), although numerous GABAergic neurons were already localized within all layers (Conti et al., 2004, Takayama and Inoue, 2010). These results suggested that although GABA may be extrasynaptically released during embryonic and postnatal development, no GABA-removal system was established in other regions. Second, GAT-1-negative GABAergic axon terminals were detected in the transient synapses in the ventral horn, although GAT-1 is localized in the majority of the presynapses of GABAergic axons in various regions of adult and developing CNS (Jursky and Nelson, 1996, Minelli et al., 2003a, Minelli et al., 2003b, Vitellaro-Zuccarello et al., 2003, Conti et al., 2004,

Takayama and Inoue, 2005, Avila et al., 2011). Third, reuptake of GABA started a little prior to the formation of GABAergic synapses, although GAT-1 appeared several days after the VGAT-expression in the cerebellar cortex (Takayama and Inoue, 2005), and at the same time in the cerebral cortex (Conti et al., 2004).

**4.3. GAT-3 in the radial glia-astrocyte lineage**

Recent studies demonstrated that radial glia, which have long radial processes, are the neural stem cells during early developmental stages (Kriegstein and Alvarez-Buylla, 2009, Costa et al., 2010, Molnar and Clowry, 2012). They proliferate by themselves within the ventricular zone, and differentiate into neurons and astrocytes. During the early stage, they symmetrically divide into stem cells, and subsequently produce neurons or neuronal progenitor cells. During the later stage, they are differentiated into astrocytes or their progenitor cells (Kriegstein and Alvarez-Buylla, 2009). In the present study, GAT-3 was not detected within the nestin-positive radial process in the dorsal horn, but was colocalized with nestin on the radial process on E13 (Fig. 10C and 10D). This result suggested that GAT-3 was not expressed in the radial glia at the early stage of proliferation and neurogenesis, and radial glia may start to express GAT-3 when they are committed to becoming glial cells during the gliogenesis stage. The change in GAT-3 immunolabeling over time was similar to that for glutamate-aspartate transporter (GLAST), one of the glutamate transporters, because GAT-3 continued to be expressed in the radial glia-astrocyte lineage during the development of the spinal cord (Shibata et al., 1997).

**Acknowledgements**

We are grateful to Makiko Moriyasu-Kuroki and Yukiji Yabiku at the Department of Molecular Anatomy for the preparation of this manuscript. We would also like to thank Hidemichi Kin, Masato Kobayashi, Yu Miyazaki, Shiori Kobayashi, Masanobu Sunagawa, Nobuhiko Okura, and Akihito Okabe at the Department of Molecular Anatomy for valuable discussion. This work was supported by Grants-in-Aid from the Ministry of Education, Culture, Sports, Science, and Technology of Japan Kiban C (No. 20500310, No. 23500413), by the Special Account Budget for Education and Research granted by the Japan Ministry of Education, and by the Takeda Science Foundation (Specified Research Grant).

**Figure legends**

**Figure 1. Immunohistochemical localization of GAT-1 and GAT-3 in the dorsal horn (A, C, D, and F) and ventral horn (B and F) of the 2-month-old mouse spinal cord.**

GAT-1-positive dots occupied the neuropil of the dorsal horn (A), but were a few in the ventral horn (arrows in B). Electron microscopic analysis demonstrated that GAT-1 immunolabeling was mainly localized within the terminals containing flat vesicles (f) and partly in the astrocytic processes (arrowheads in C). GAT-3 immunolabeling was diffusely distributed in the neuropil of both dorsal (D) and ventral horns (E). Electron microscopic pictures demonstrated that GAT-3 was localized within astrocyte processes (arrowheads in F).

I-IV: lamina I-IV, s: presynapses containing spherical vesicles, triangles: cell bodies of motor neurons. Scale bars: A, B, D, E: 10 μm, C, E: 1 μm.

**Figure 2. Developmental localization of GAT-1 in the embryonic spinal cord on E12 (A), E13 (B), E15 (C), E16 (D), and E18 (E) at the lower magnification.**

Weak GAT-1 immunolabeling was detected in the marginal zone (MZ) and white matter (A-C). In the dorsal horn (DH), faint immunolabeling was detected on E15 (C), and intensity of the GAT-1 immunolabeling increased after E16 (D and E). By contrast, in the ventral horn (VH), GAT-1 immunolabeling was faint (B-E). Squares indicate the location of the higher magnification photographs in Figure 3. AF: anterior funiculus, LF: lateral funiculus, ML: mantle layer, PF: posterior funiculus, VZ: ventricular zone. Scale bar: 100 μm.

**Figure 3. Embryonic development of GAT-1 localization in the ventral part (A-D) and**

**dorsal part (E-H) on E13 (A), E15 (B, E, and F), E16 (C and G), and E18 (D and H) at the higher magnification.**

In the ventral part, only a few GAT-1-positive dots (arrows) were localized within the anterior funiculus (AF) and the ventral horn (VH). In the dorsal horn (DH), a few GAT-1-positive dots were detected at the axons (arrowheads) on E13 (F), and the density of the GAT-1-positive varicosities increased mainly in the lamina III after E16 (G and H). Triangles: cell bodies of large motor neurons, PF: posterior funiculus, I-III: lamina I- III. Scale bar: 10 μm.

**Figure 4. Electron microscopic localization of GAT-1 in the dorsal horn on E18.**

GAT-1 was localized within the presynapse, which formed synapses (asterisks in A-C), and axons (Ax in C). A small amount of immunolabeling was detected within processes of astrocytes (arrowheads in A and B). Scale bar: 1 μm.

**Figure 5. Postnatal development of GAT-1 localization in the ventral horn (A-D) and dorsal horn (E-H) on P0 (A and E), P7 (B and F), P14 (C and G), and P21 (D and H) at the higher magnification.**

In the ventral horn, a few GAT-1-positive dots (arrows) were detected, and the neuropil was weakly stained (A-D). By contrast, in the dorsal horn, GAT-1 immunolabeling was dense and increased in intensity during development (E-H). GAT-1-positive dots were densely detected mainly in the lamina III (III) on P0 (E), lamina I (I) and III (III) on P7 (F), and lamina I to III (I, II, III) after P14 (G and H). Triangles: cell bodies of motor neurons. Scale bar: 10 μm.

**Figure 6. Developmental localization of GAT-3 in the embryonic spinal cord on E12 (A), E13 (B), E15 (C), E16 (D), and E18 (E) at the lower magnification.**

GAT-3 immunolabeling was first detected at the radial fibers in the ventral region on E12 (A), in the ventral half on E13 (B), and throughout the spinal cord on E15 (C). GAT-3 immunolabeling exhibited small fragments on E16 (D) and E18 (E). Squares indicate the location of the higher magnification photographs in Figure 7. AF: anterior funiculus, cc: central canal, DH: dorsal horn, LF: lateral funiculus, ML: mantle layer, MZ: marginal zone, PF: posterior funiculus, VH: ventral horn, VZ: ventricular zone. Scale bar: 100 μm.

**Figure 7. Embryonic development of GAT-3 localization in the ventral part (A-D) and dorsal part (E-H) on E12 (A), E13 (B), E15 (C and F), E16 (D and G) and E18 (E and H) at the higher magnification.**

Radial fibers (arrows) were clearly discernible by GAT-3 immunostaining until E15 (A-C). In the ventral horn (VH) on E15, many branches were detected (C). After E16, radial processes were unclear and numerous fragments or particle-like-profiles occupied the neuropil (D and E). In the dorsal horn (DH), radial processes (arrows) were first detected on E15 (F), and the shapes of GAT-3-positive structure gradually changed to fragment-like-profiles on E16 (G), and fine dots scattered in laminar II and III on E18 (H). Triangles: cell bodies of motor neurons, cc: central canal, LF: lateral funiculus, ML: mantle layer, MZ: marginal zone, VZ: ventricular zone. Scale bar: 10 μm.

**Figure 8. Electron microscopic localization of GAT-3 in the dorsal horn on E15 (A-D) and E18 (E and F).**

GAT-3 immunolabeling was detected within the radial fibers and their short branches (arrows) invading into the inter-neuronal space on E15 (A-D). On E18, GAT-3 immunolabeling was localized near the cell membrane of astrocyte (As) processes, and the GAT-3-positive processes (arrows) filled up the inter-neuronal spaces and often attached or surrounded the symmetric and asymmetric synapses (asterisks in E and F). Scale bars: 1 μm.

**Figure 9. Postnatal development of GAT-3 localization in the ventral horn (A-D) and dorsal horn (E-H) on P0 (A and E), P7 (B and F), P14 (C and G), and P21 (D and H) at the higher magnification.**

On P0, GAT-3-positive fine dots or short fibrous profiles occupied the neuropil region in the ventral horn (A). After P7, the immunolabeling increased in density (B-D). In the dorsal horn, GAT-3 immunolabeling was detected in all lamina (I-III) (E-H). Density of the GAT-3-positive dots gradually increased until P21 (F-H). Triangles: cell bodies of the motor neurons. Scale bar: 10 μm.

**Figure 10. Double labeling of GAT-1 (red in A, B, and F) and GAT-3 (red in C, D, and E) with synaptic and glial markers, VGAT (green in A, B, and F) and nestin (green in C, D, and E) on E13 (C and D), E15 (E), and E18 (A, B, and F).**

In the dorsal horn on E18, many of the GAT-1-positive dots were merged with fine

VGAT-positive dots (yellow), but GAT-1 single positive dots (red) were also detected (A). By contrast, in the ventral horn, the majority of the VGAT-positive dots were not colocalized with GAT-1 immunolabeling; few GAT-1-positive dots were merged with VGAT (circles in B). On E13, the trunks of the GAT-3-positive fibers were colocalized with nestin-positive fibers in the ventral horn (C). The radial fibers were nestin-positive but GAT-3-negative (D). In the dorsal horn on E15, many GAT-3-positive profiles were nestin-negative, and a few nestin-positive fibers were colocalized with GAT-3 immunolabeling (arrows in E). On E18, some of the VGAT-positive dots were attached to the GAT-3-positive fibrous profiles, but they were not merged (F). I-IV: lamina I-IV, triangles: cell bodies of the motor neurons. Scale bar: 10 μm.

**Figure 11. Schematic illustrations of changes in GABA-removal system.**

Before synapses are formed, GABA, released from the axons and growth cones of GABAergic neurons, may be transported into the processes of radial glia (RG) by GAT-3 (A). In the dorsal horn, GABAergic synapses were formed during late embryonic and postnatal development. In the immature GABAergic synapses, GABA may be reuptaken into presynapses by GAT-1 and transported into the developing astrocytes by GAT-3. After astrocytic processes seal the GABAergic synapse, GABA in the synaptic cleft may be removed by GAT-1 and GAT-3 into presynapses and neighboring astrocyte processes, respectively (B). In the ventral horn, many GABAergic synapses were transiently formed and disappeared during postnatal development, namely transient GABAergic synapse. In the transient GABAergic synapses, GABA may be

transported into the developing astrocytic processes by GAT-3, but may not be reuptaken into presynapse (C). The fate of this transient GABAergic synapse was not revealed, but several studies suggested the transformation into the glycinergic synapses.

1: GAT-1, 3: GAT-3, As: astrocytes, Gly: glycine, R: $GABA_A$ or glycine receptor.

**Table 1. Antibody characterization.**

| **Antigen** | **Immunogen** | **Manufacturer, species, antibody type** | **Dilution** |
|---|---|---|---|
| GABA transporter -1 (GAT-1) | Synthetic peptide, aa 588-599 of rat GAT-1 | Sigma-Aldrich (SAB2102222, St. Louis MO), rabbit, polyclonal | 1:2000 |
| GABA transporter -3 (GAT-3) | Synthetic peptide, aa 607-627 of rat GAT-3 | Sigma-Aldrich (G8407, St. Louis MO), rabbit, polyclonal | 1:2000 |
| Nestin | nestin purified from embryonic rat spinal cord | Millipore (MAB353, Billerica, MA), mouse, monoclonal (IgG1) | 1:2000 |
| VGAT | Synthetic peptide, aa 1022-1042 of mouse VGAT | Guinea pig, polyclonal (Takayama and Inoue, 2004a) | 1 μg/ml |

## References


Allain AE, Bairi A, Meyrand P, Branchereau P (2006) Expression of the glycinergic system during the course of embryonic development in the mouse spinal cord and its co-localization with GABA immunoreactivity. J Comp Neurol 496:832-846.

Avila MA, Real MA, Guirado S (2011) Patterns of GABA and GABA Transporter-1 immunoreactivities in the developing and adult mouse brain amygdala. Brain Res 1388:1-11.

Ben-Ari Y (2002) Excitatory actions of gaba during development: the nature of the nurture. Nat Rev Neurosci 3:728-739.

Ben-Ari Y, Gaiarsa JL, Tyzio R, Khazipov R (2007) GABA: a pioneer transmitter that excites immature neurons and generates primitive oscillations. Physiol Rev 87:1215-1284.

Borden LA (1996) GABA transporter heterogeneity: pharmacology and cellular localization. Neurochem Int 29:335-356.

Chiu CS, Brickley S, Jensen K, Southwell A, McKinney S, Cull-Candy S, Mody I, Lester HA (2005) GABA transporter deficiency causes tremor, ataxia, nervousness, and increased GABA-induced tonic conductance in cerebellum. J Neurosci 25:3234-3245.

Conti F, Minelli A, Melone M (2004) GABA transporters in the mammalian cerebral cortex: localization, development and pathological implications. Brain Res Brain Res Rev 45:196-212.

Costa MR, Gotz M, Berninger B (2010) What determines neurogenic competence in glia? Brain Res Rev 63:47-59.

Egawa K, Kitagawa K, Inoue K, Takayama M, Takayama C, Saitoh S, Kishino T, Kitagawa M, Fukuda A (2012) Decreased tonic inhibition in cerebellar granule cells causes motor dysfunction in a mouse model of Angelman syndrome. Sci Transl Med 4:163ra157.

Evans JE, Frostholm A, Rotter A (1996) Embryonic and postnatal expression of four gamma-aminobutyric acid transporter mRNAs in the mouse brain and leptomeninges. J Comp Neurol 376:431-446.

Gadea A, Lopez-Colome AM (2001) Glial transporters for glutamate, glycine, and GABA: II. GABA transporters. J Neurosci Res 63:461-468.

Gao BX, Stricker C, Ziskind-Conhaim L (2001) Transition from GABAergic to glycinergic synaptic transmission in newly formed spinal networks. J Neurophysiol 86:492-502.

Gao BX, Ziskind-Conhaim L (1995) Development of glycine- and GABA-gated currents in rat spinal motoneurons. J Neurophysiol 74:113-121.

Hsu SM, Raine L, Fanger H (1981) Use of avidin-biotin-peroxidase complex (ABC) in immunoperoxidase techniques: a comparison between ABC and unlabeled antibody (PAP) procedures. J Histochem Cytochem 29:577-580.

Itouji A, Sakai N, Tanaka C, Saito N (1996) Neuronal and glial localization of two GABA transporters (GAT1 and GAT3) in the rat cerebellum. Brain Res Mol Brain Res 37:309-316.

Jin XT, Galvan A, Wichmann T, Smith Y (2011a) Localization and Function of GABA Transporters

GAT-1 and GAT-3 in the Basal Ganglia. Front Syst Neurosci 5:63.

Jin XT, Pare JF, Smith Y (2011b) Differential localization and function of GABA transporters, GAT-1 and GAT-3, in the rat globus pallidus. Eur J Neurosci 33:1504-1518.

Jursky F, Nelson N (1996) Developmental expression of GABA transporters GAT1 and GAT4 suggests involvement in brain maturation. J Neurochem 67:857-867.

Jursky F, Nelson N (1999) Developmental expression of the neurotransmitter transporter GAT3. J Neurosci Res 55:394-399.

Jursky F, Tamura S, Tamura A, Mandiyan S, Nelson H, Nelson N (1994) Structure, function and brain localization of neurotransmitter transporters. J Exp Biol 196:283-295.

Kanner BI (1994) Sodium-coupled neurotransmitter transport: structure, function and regulation. J Exp Biol 196:237-249.

Kosaka Y, Kin H, Tatetsu M, Uema I, Takayama C (2012) Distinct development of GABA system in the ventral and dorsal horns in the embryonic mouse spinal cord. Brain Res 1486:39-52.

Kriegstein A, Alvarez-Buylla A (2009) The glial nature of embryonic and adult neural stem cells. Annu Rev Neurosci 32:149-184.

Liu GX, Cai GQ, Cai YQ, Sheng ZJ, Jiang J, Mei Z, Wang ZG, Guo L, Fei J (2007a) Reduced anxiety and depression-like behaviors in mice lacking GABA transporter subtype 1. Neuropsychopharmacology 32:1531-1539.

Liu GX, Liu S, Cai GQ, Sheng ZJ, Cai YQ, Jiang J, Sun X, Ma SK, Wang L, Wang ZG, Fei J (2007b) Reduced aggression in mice lacking GABA transporter subtype 1. J Neurosci Res 85:649-655.

Liu Y, Wu Y, Lee JC, Xue H, Pevny LH, Kaprielian Z, Rao MS (2002) Oligodendrocyte and astrocyte development in rodents: an in situ and immunohistological analysis during embryonic development. Glia 40:25-43.

Macdonald RL, Olsen RW (1994) GABAA receptor channels. Annu Rev Neurosci 17:569-602.

McCarthy MM, Auger AP, Perrot-Sinal TS (2002) Getting excited about GABA and sex differences in the brain. Trends Neurosci 25:307-312.

Minelli A, Alonso-Nanclares L, Edwards RH, DeFelipe J, Conti F (2003a) Postnatal development of the vesicular GABA transporter in rat cerebral cortex. Neuroscience 117:337-346.

Minelli A, Barbaresi P, Conti F (2003b) Postnatal development of high-affinity plasma membrane GABA transporters GAT-2 and GAT-3 in the rat cerebral cortex. Brain Res Dev Brain Res 142:7-18.

Minelli A, Brecha NC, Karschin C, DeBiasi S, Conti F (1995) GAT-1, a high-affinity GABA plasma membrane transporter, is localized to neurons and astroglia in the cerebral cortex. J Neurosci 15:7734-7746.

Minelli A, DeBiasi S, Brecha NC, Zuccarello LV, Conti F (1996) GAT-3, a high-affinity GABA plasma membrane transporter, is localized to astrocytic processes, and it is not confined to the vicinity of GABAergic synapses in the cerebral cortex. J Neurosci 16:6255-6264.

Molnar Z, Clowry G (2012) Cerebral cortical development in rodents and primates. Prog Brain Res

195:45-70.

Morara S, Brecha NC, Marcotti W, Provini L, Rosina A (1996) Neuronal and glial localization of the GABA transporter GAT-1 in the cerebellar cortex. Neuroreport 7:2993-2996.

Nabekura J, Katsurabayashi S, Kakazu Y, Shibata S, Matsubara A, Jinno S, Mizoguchi Y, Sasaki A, Ishibashi H (2004) Developmental switch from GABA to glycine release in single central synaptic terminals. Nat Neurosci 7:17-23.

Olsen RW, Tobin AJ (1990) Molecular biology of GABAA receptors. Faseb J 4:1469-1480.

Owens DF, Kriegstein AR (2002) Is there more to GABA than synaptic inhibition? Nat Rev Neurosci 3:715-727.

Peters A, Palay SL, Webster HD (1991) The fine structure of the nervous system. New York: Oxford University Press.

Phelps PE, Alijani A, Tran TS (1999) Ventrally located commissural neurons express the GABAergic phenotype in developing rat spinal cord. J Comp Neurol 409:285-298.

Radian R, Ottersen OP, Storm-Mathisen J, Castel M, Kanner BI (1990) Immunocytochemical localization of the GABA transporter in rat brain. J Neurosci 10:1319-1330.

Represa A, Ben-Ari Y (2005) Trophic actions of GABA on neuronal development. Trends Neurosci 28:278-283.

Schaffner AE, Behar T, Nadi S, Smallwood V, Barker JL (1993) Quantitative analysis of transient GABA expression in embryonic and early postnatal rat spinal cord neurons. Brain Res Dev Brain Res 72:265-276.

Shi J, Cai Y, Liu G, Gong N, Liu Z, Xu T, Wang Z, Fei J (2012) Enhanced learning and memory in GAT1 heterozygous mice. Acta Biochim Biophys Sin (Shanghai) 44:359-366.

Shibata T, Yamada K, Watanabe M, Ikenaka K, Wada K, Tanaka K, Inoue Y (1997) Glutamate transporter GLAST is expressed in the radial glia-astrocyte lineage of developing mouse spinal cord. J Neurosci 17:9212-9219.

Sibilla S, Ballerini L (2009) GABAergic and glycinergic interneuron expression during spinal cord development: dynamic interplay between inhibition and excitation in the control of ventral network outputs. Prog Neurobiol 89:46-60.

Takayama C (2005) GABAergic signaling in the developing cerebellum. In: GABA in autism and related disorders, vol. 71 (Dhossche, D. M., ed), pp 63-94 San Diego: Elsevier.

Takayama C, Inoue Y (2004a) Extrasynaptic localization of GABA in the developing mouse cerebellum. Neurosci Res 50:447-458.

Takayama C, Inoue Y (2004b) Morphological development and maturation of the GABAergic synapses in the mouse cerebellar granular layer. Brain Res Dev Brain Res 150:177-190.

Takayama C, Inoue Y (2004c) Transient expression of GABA(A) receptor alpha2 and alpha3 subunits in differentiating cerebellar neurons. Brain Res Dev Brain Res 148:169-177.

Takayama C, Inoue Y (2005) Developmental expression of GABA transporter-1 and 3 during formation of the GABAergic synapses in the mouse cerebellar cortex. Brain Res Dev Brain

Res 158:41-49.

Takayama C, Inoue Y (2006) Developmental localization of potassium chloride co-transporter 2 in granule cells of the early postnatal mouse cerebellum with special reference to the synapse formation. Neuroscience 143:757-767.

Takayama C, Inoue Y (2007) Developmental localization of potassium chloride co-transporter 2 (KCC2) in the Purkinje cells of embryonic mouse cerebellum. Neurosci Res 57:322-325.

Takayama C, Inoue Y (2010) Developmental localization of potassium chloride co-transporter 2 (KCC2), GABA and vesicular GABA transporter (VGAT) in the postnatal mouse somatosensory cortex. Neurosci Res 67:137-148.

Tran TS, Alijani A, Phelps PE (2003) Unique developmental patterns of GABAergic neurons in rat spinal cord. J Comp Neurol 456:112-126.

Vitellaro-Zuccarello L, Calvaresi N, De Biasi S (2003) Expression of GABA transporters, GAT-1 and GAT-3, in the cerebral cortex and thalamus of the rat during postnatal development. Cell Tissue Res 313:245-257.

Wu WL, Ziskind-Conhaim L, Sweet MA (1992) Early development of glycine- and GABA-mediated synapses in rat spinal cord. J Neurosci 12:3935-3945.

Xu YF, Cai YQ, Cai GQ, Jiang J, Sheng ZJ, Wang ZG, Fei J (2008) Hypoalgesia in mice lacking GABA transporter subtype 1. J Neurosci Res 86:465-470.

Zink M, Vollmayr B, Gebicke-Haerter PJ, Henn FA (2009) Reduced expression of GABA transporter GAT3 in helpless rats, an animal model of depression. Neurochem Res 34:1584-1593.

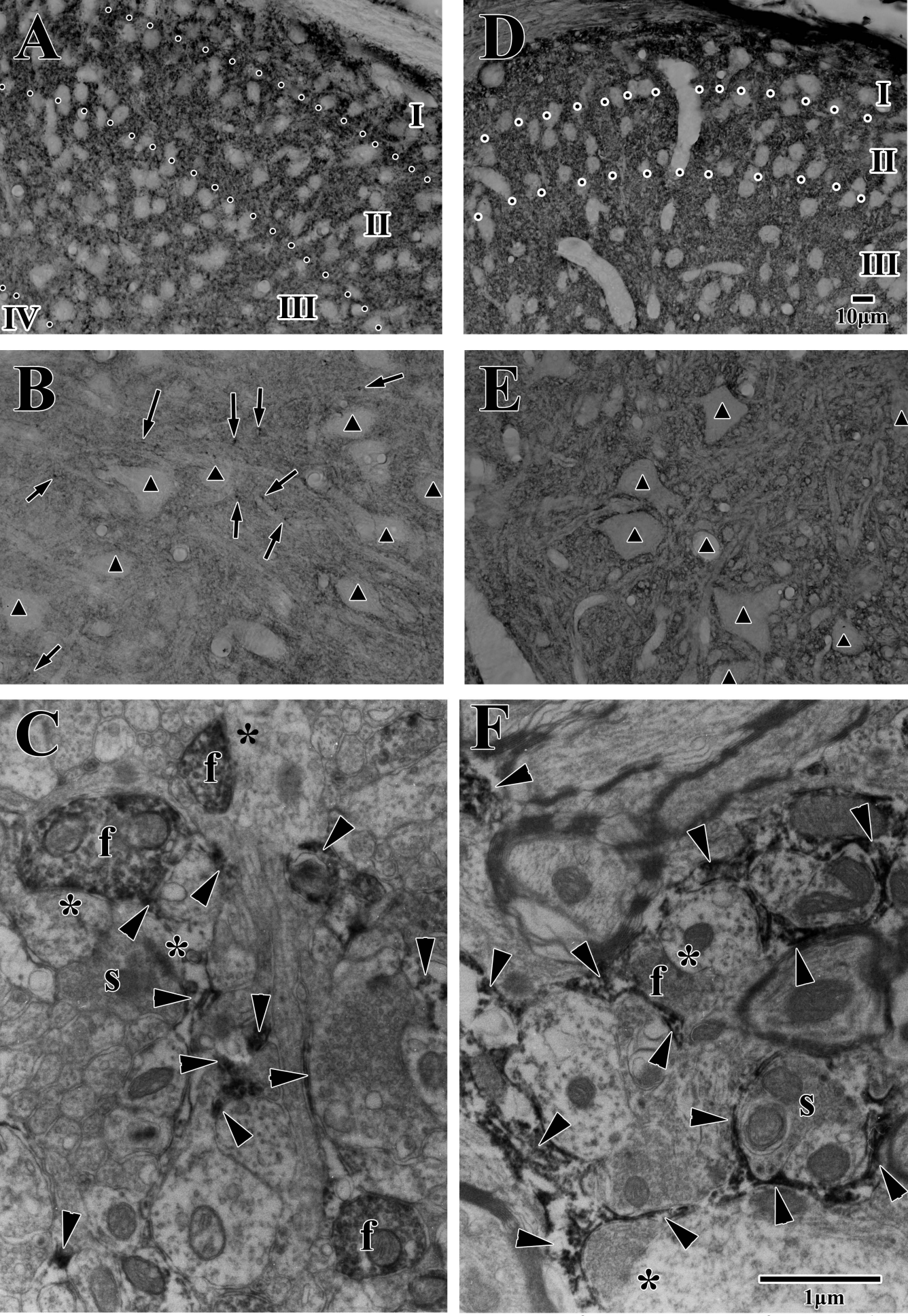


Kim et al. Figure1

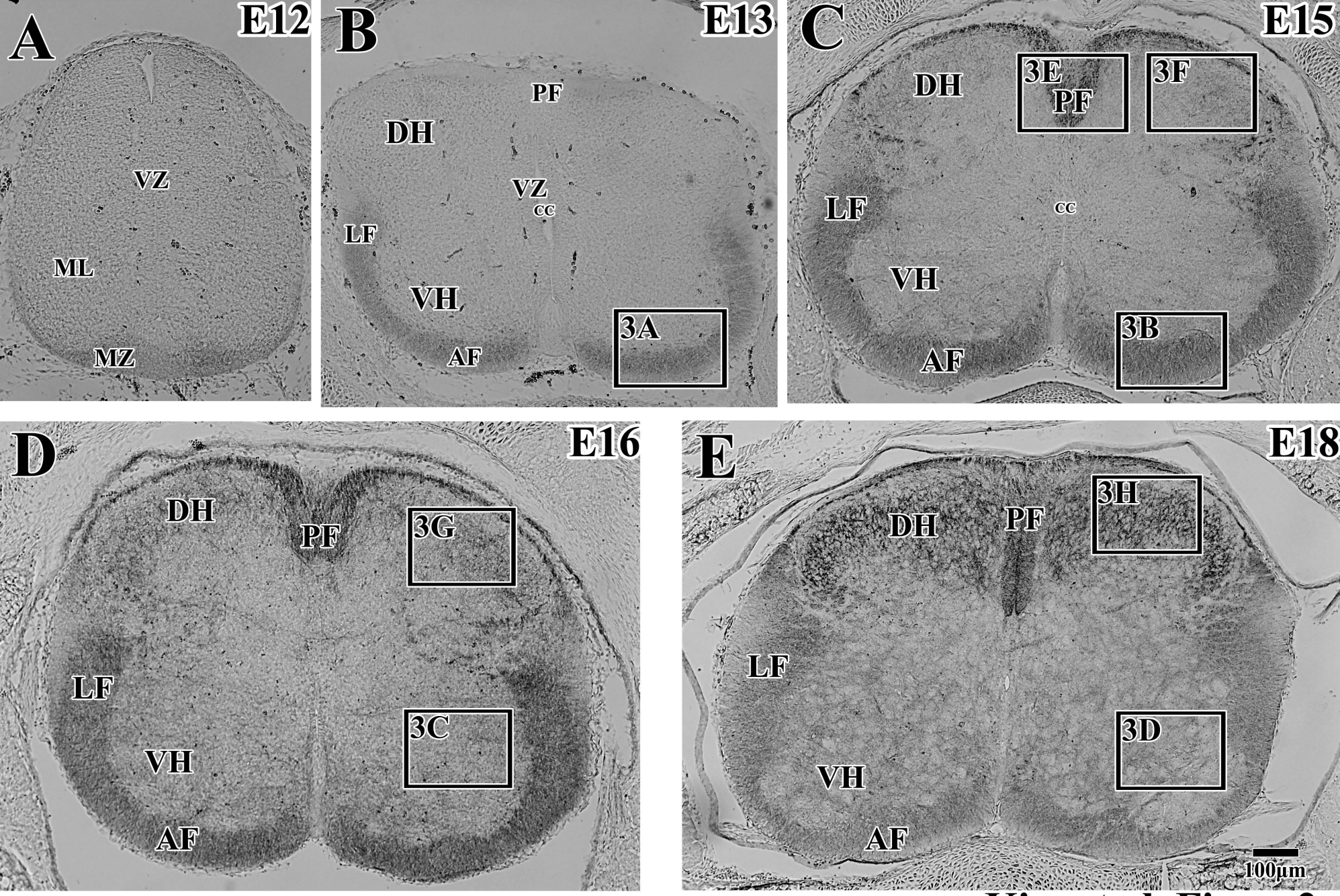


Kim et al. Figure2

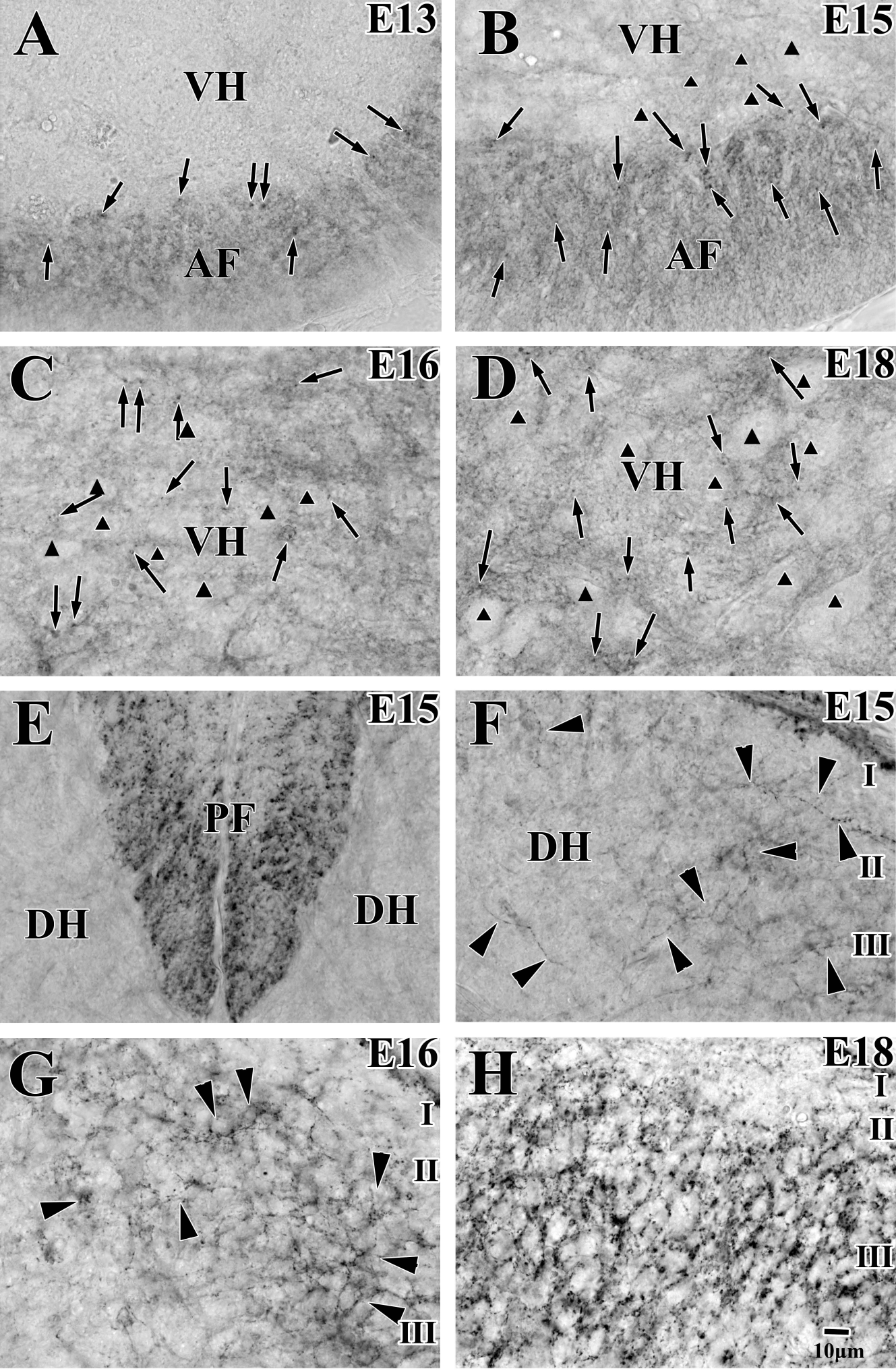


Kim et al. Figure3

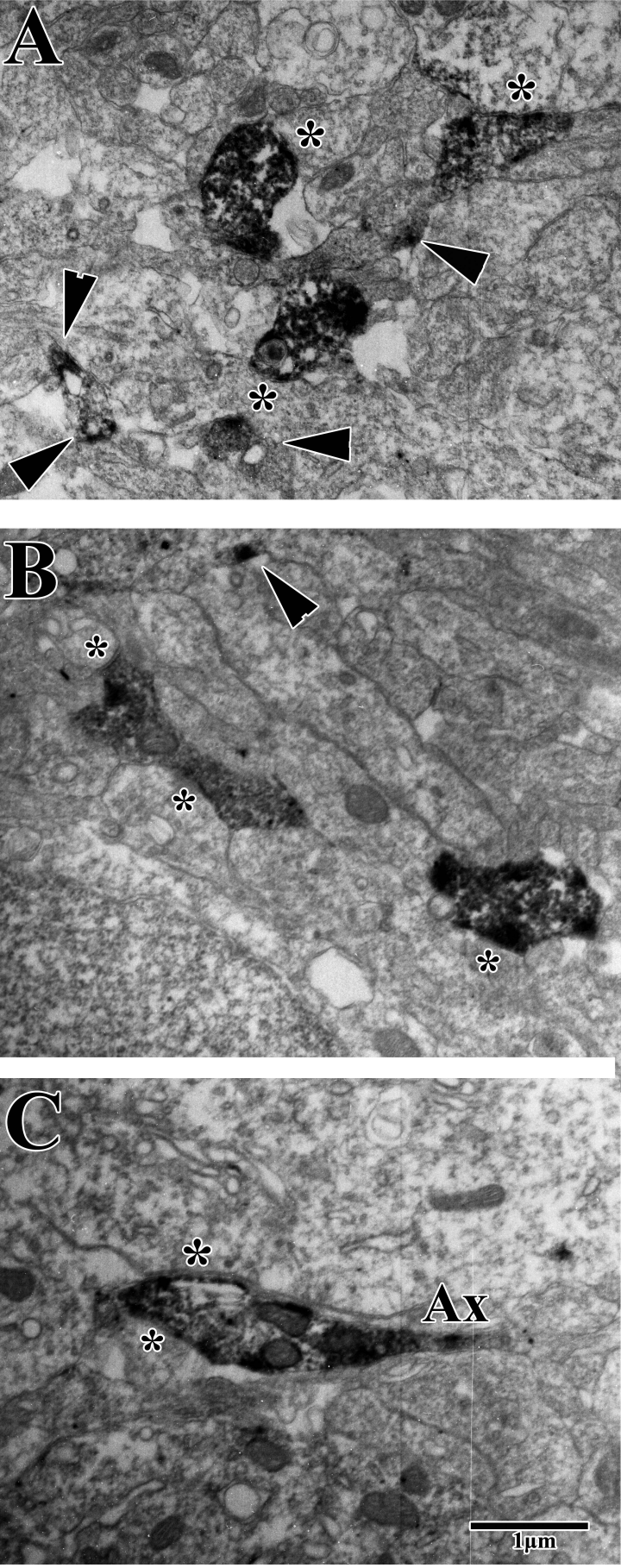


Kim et al. Figure4

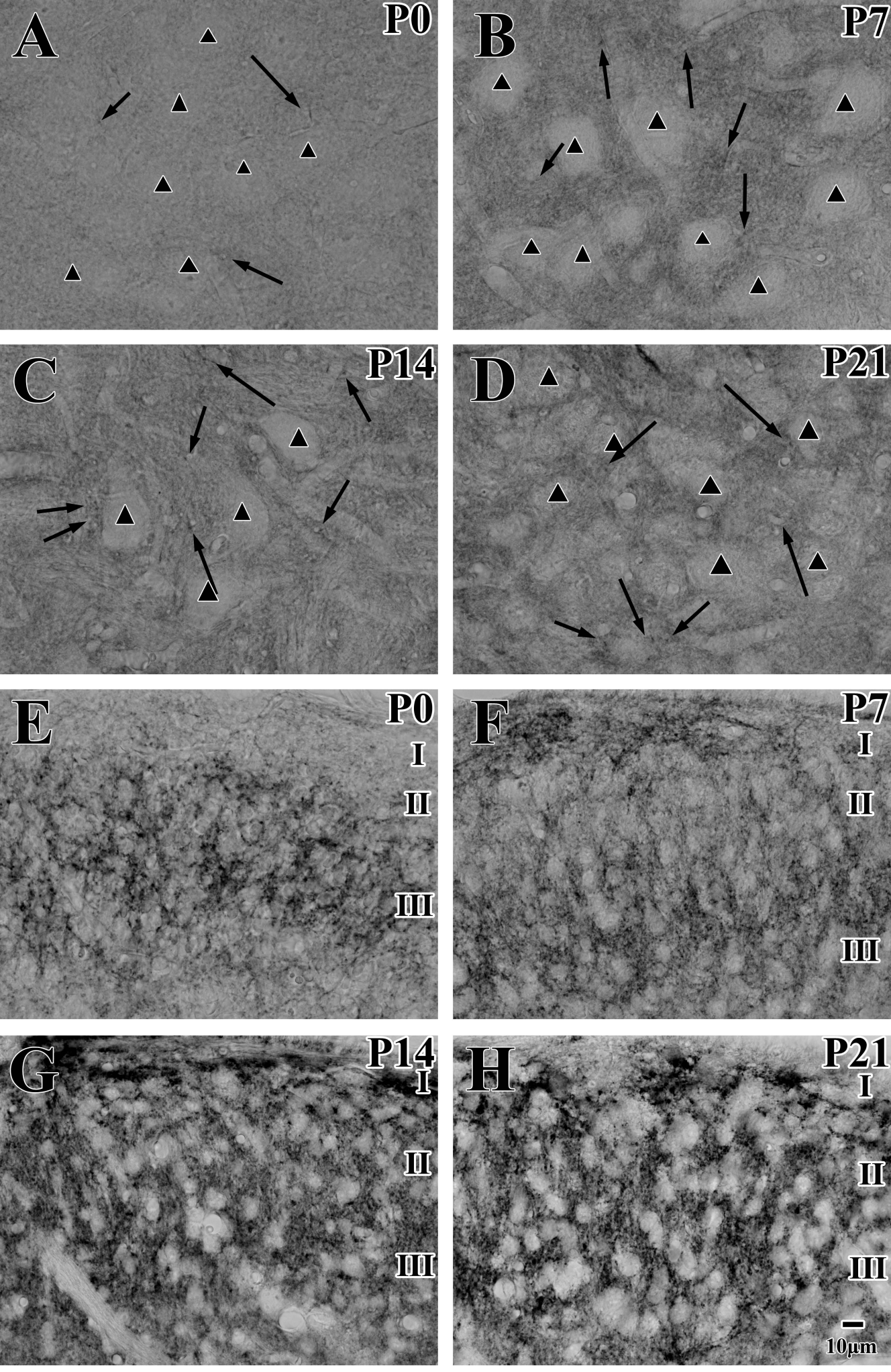


Kim et al. Figure5

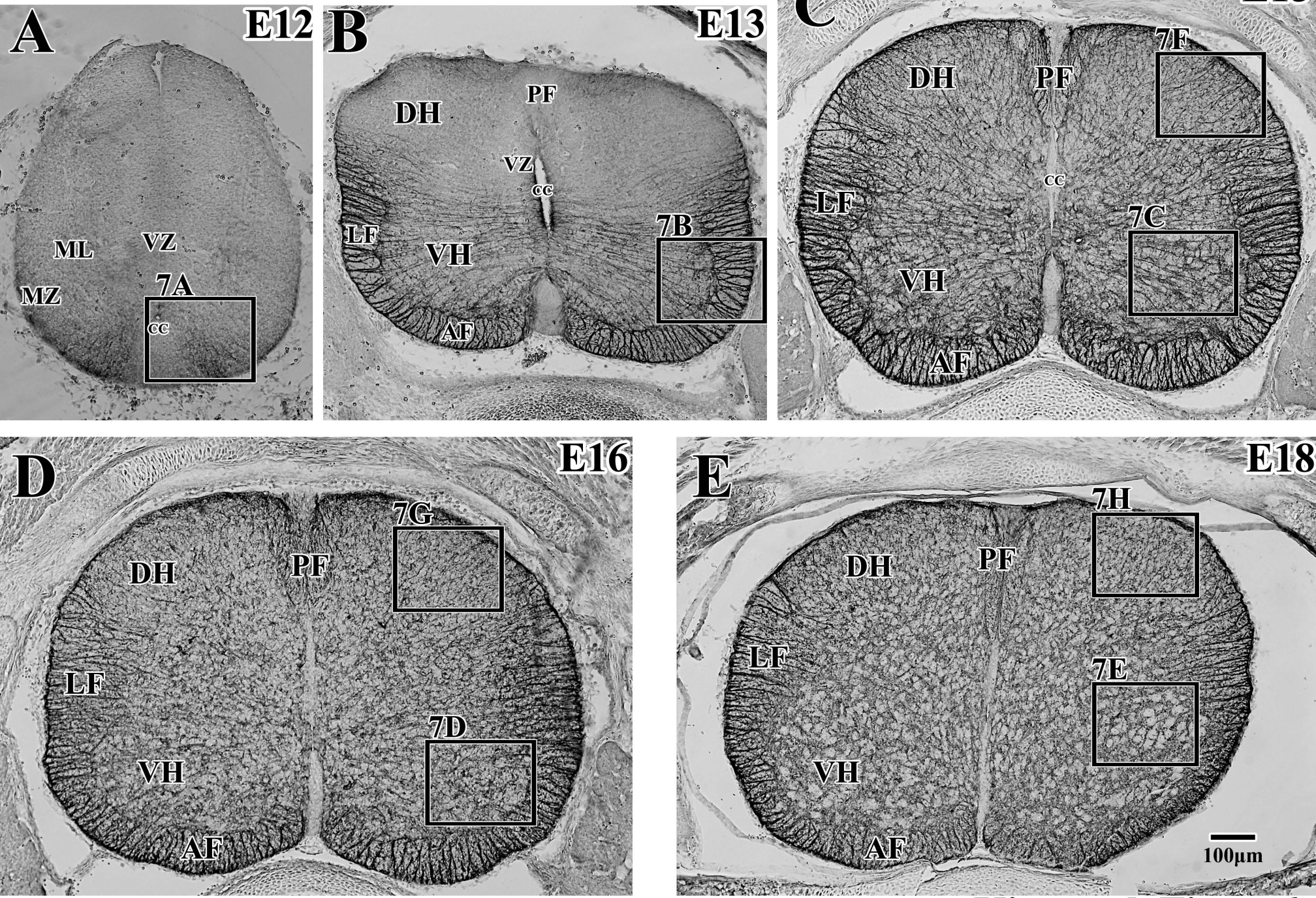


Kim et al. Figure6

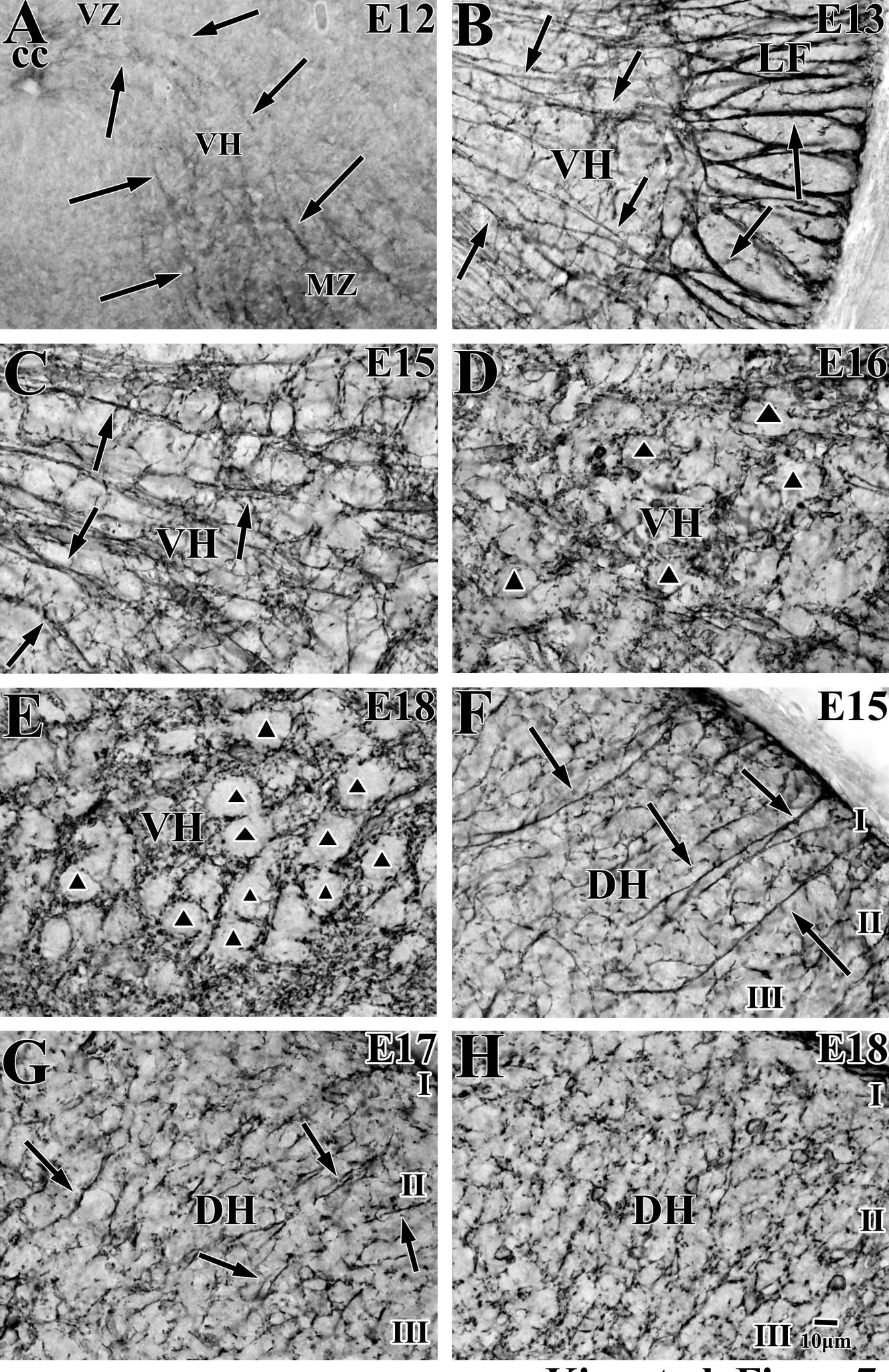


Kim et al. Figure7

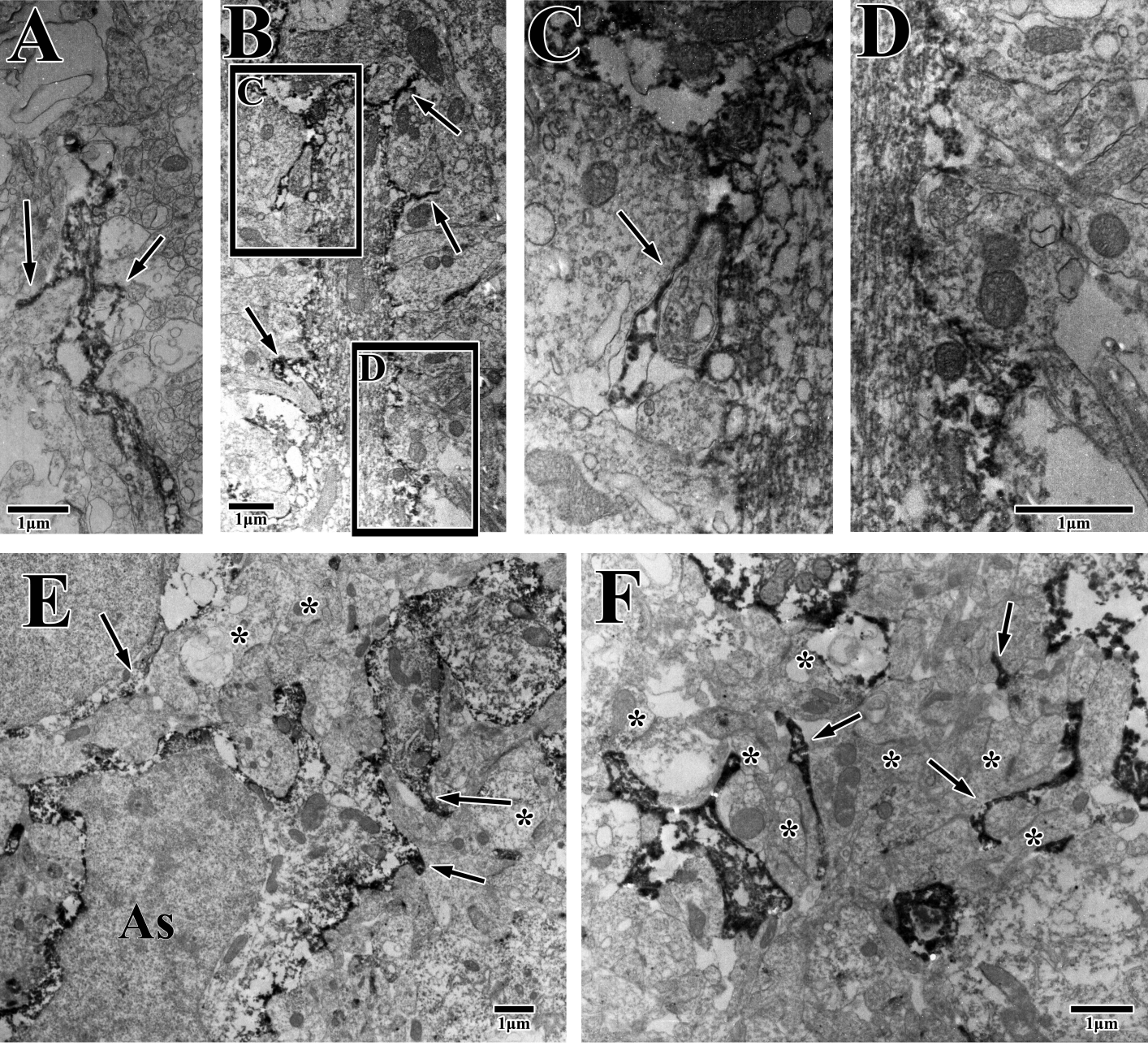


Kim et al. Figure8

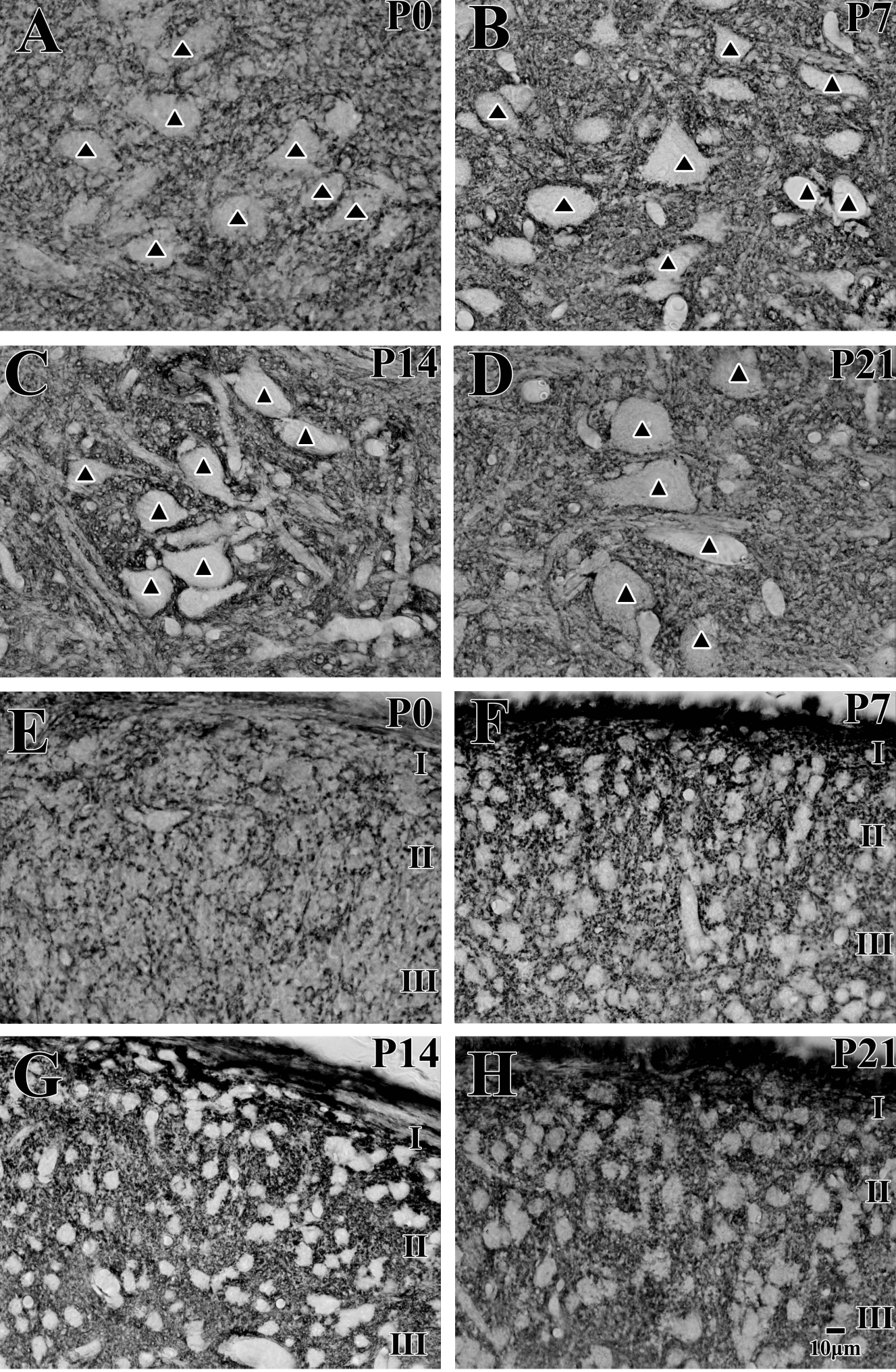


Kim et al. Figure9

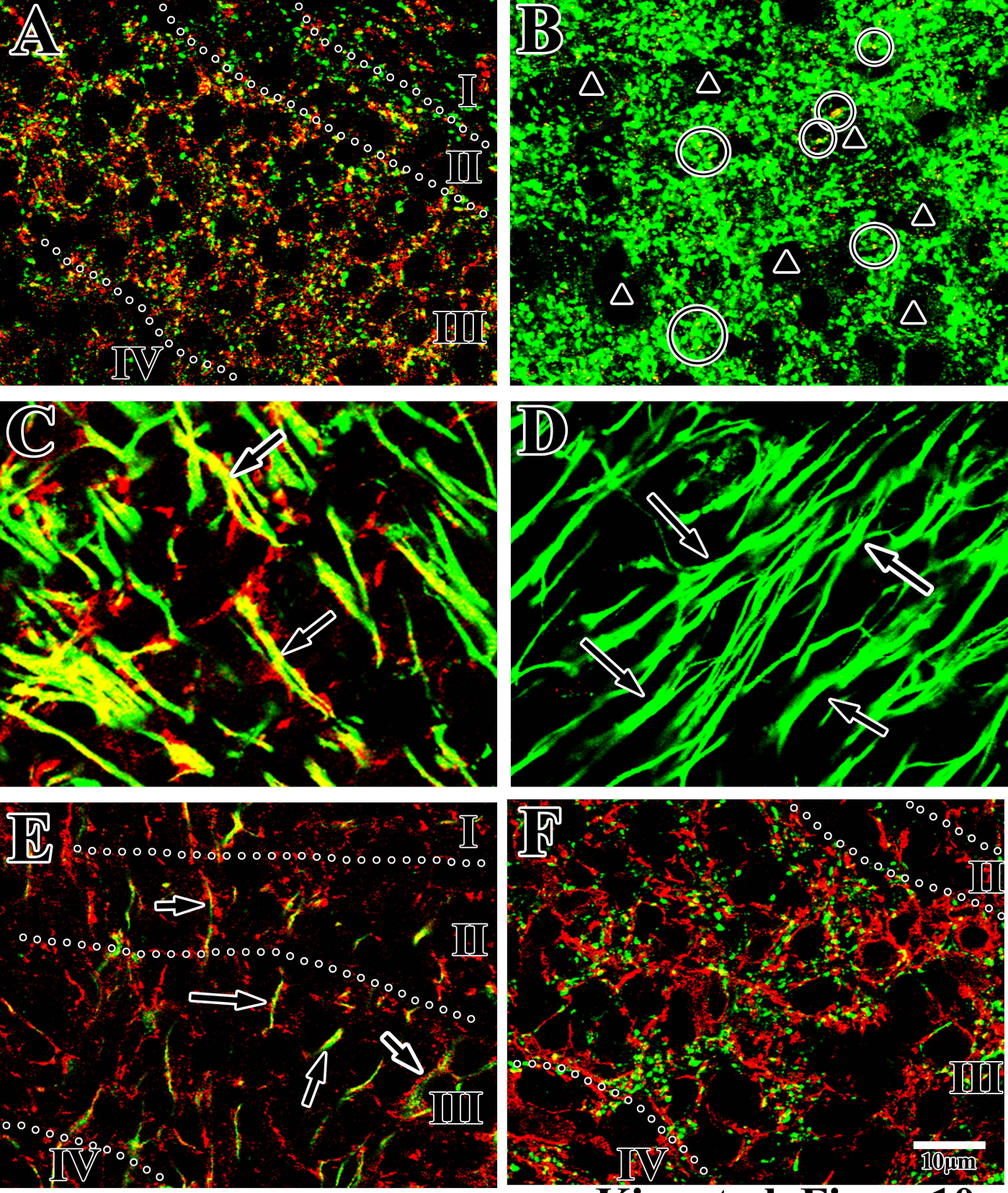


Kim et al. Figure10

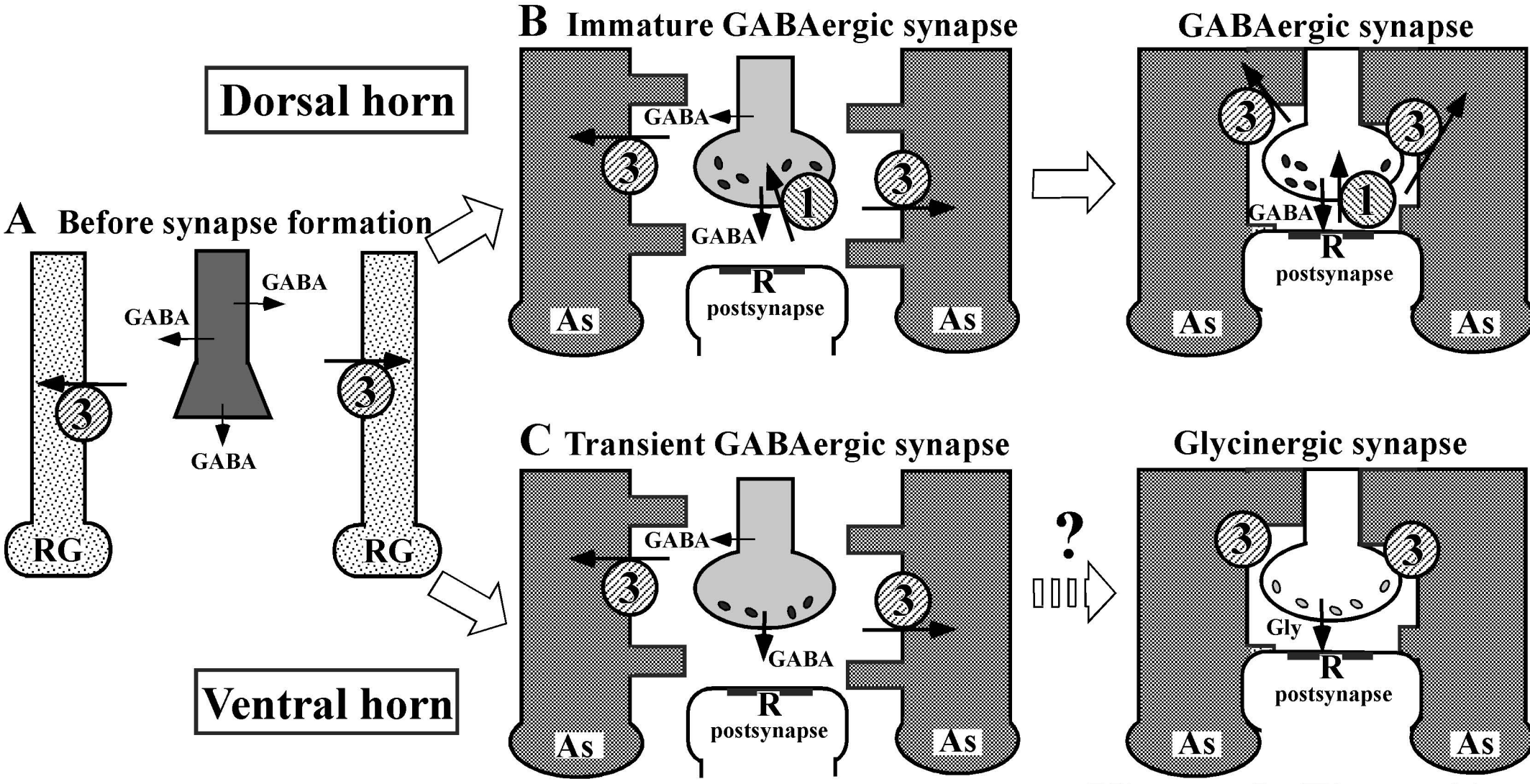


Kim et al. Figure 11

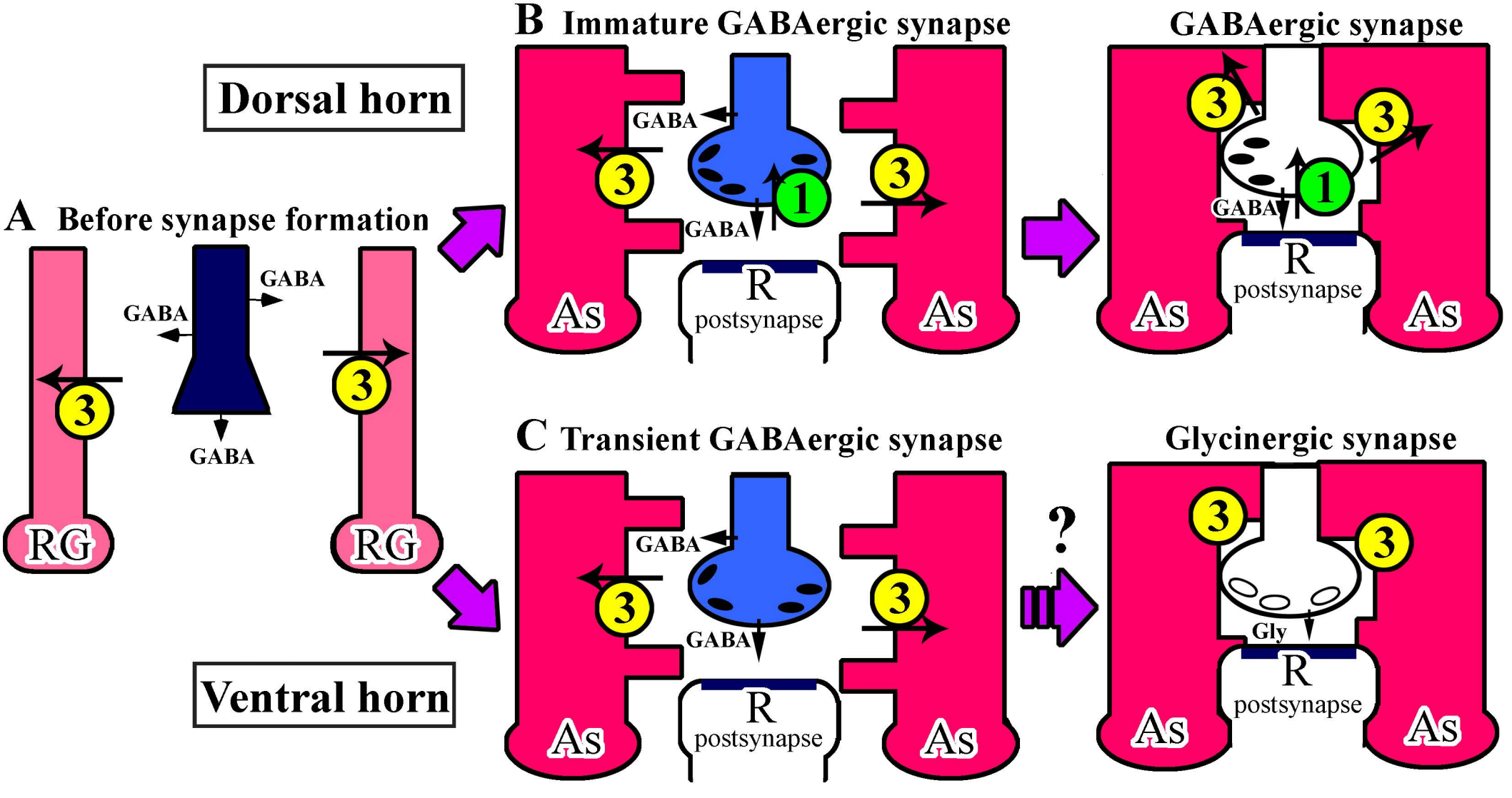
Dorsal horn
A Before synapse formation
GABA
GABA
GABA
3
RG
RG
B Immature GABAergic synapse
GABA
3
GABA
1
3
As
R
postsynapse
As
GABAergic synapse
3
3
GABA
1
R
postsynapse
As
As
C Transient GABAergic synapse
GABA
3
GABA
3
As
R
postsynapse
As
?
Glycinergic synapse
3
3
Gly
R
postsynapse
As
As
Ventral horn